

# Structure Response to Trench and Road Blasting

Vitor L. Rosenhaim

*M.S. Graduate Student, Mineral and Explosives Engineering, New Mexico Institute of Mining and Technology, Socorro, NM, USA*

Charles H. Dowding

*Professor of Civil and Environmental Engineering, Northwestern University, Evanston, IL, USA*

Catherine T. Aimone-Martin

*Professor of Mineral and Civil Engineering, New Mexico Institute of Mining and Technology, Socorro, NM, USA*

**ABSTRACT:** Crack and structural response to construction trench blasting was measured in a wood-frame house with a stucco exterior. Blasts at distances between 232 m to 368 m produced peak particle velocities (PPV) and air blast over pressures (AB) of 9 mm/sec and 0.02 kPa (123 dB), respectively. Structural response velocities were measured at an upper corner and two mid-walls, as were changes in the width of a crack at a window corner in the east midwall. Structure responses were correlated with PPV and AB, which arrived simultaneously, which complicated the distinction between the two. Crack responses were correlated with long-term changes in temperature and humidity as well as PPV and AB. Wall strains from out of plane bending and in-plane shear were computed from upper corner structure response and compared to failure strains for drywall. As has been found in other studies, calculated strains were far lower than those required to crack drywall and environmentally induced crack response from temperature and humidity was far greater than that caused by blast induced ground motion or airblast overpressures.

## 1 INSTRUMENTATION TO MEASURE STRUCTURE RESPONSE

Figures 1 and 2 show the instrumentation locations within, and exterior to, the structure. The location of the interior, single component velocity transducers placed in the upper (S2) corner, lower (S1) corner, and at the mid-wall in the living room east and north walls are indicated in Figure 1. LARCOR™ multi-component seismographs were used to digitally record four channels of seismic data. The exterior (master) unit consisted of a triaxial geophone and an airblast microphone. The geophone, buried 150 mm in depth, was oriented so that the radial, R, and transverse, T, components were perpendicular and parallel respectively to the east wall containing the instrumented crack. This orientation is based upon recording motions that are parallel to one of the house's translation axes rather than the traditional direction relative to the vibration source. The airblast microphone was installed 250 mm above the ground surface and used to record the pressure pulses transmitted through the air.

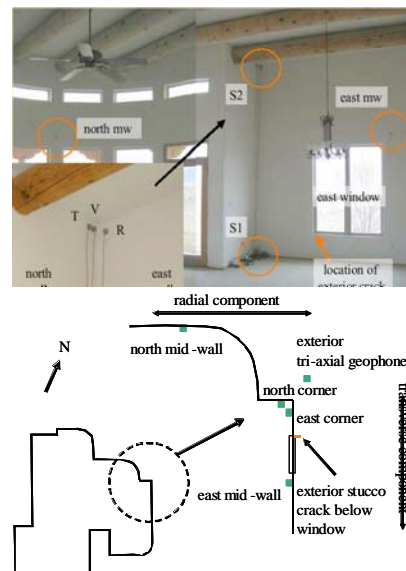


Figure 1. Plan view of instrumented house (top) and locations of velocity transducers to measure structural response (bottom).

The three seismographs and field computer were connected in series, with the exterior seismograph acting as the master (triggering) unit and all other systems as slave units. The Kaman gage system was programmed to sample crack displacement every hour in response to environmental changes. Upon triggering, the master seismograph delivered a 1 volt pulse via the serial cable to activate and begin recording dynamic data during blasting events. This produced seismograph and dynamic crack/null gage records that were time-correlated to the nearest 0.001 second, which is critical for analysis of structural and crack response.

## 2 GROUND MOTION AND AIRBLAST ENVIRONMENT

Blasting, ground motion and airblast data are given in Table 1. Figure 3 shows blast locations as shot layouts for trench and road blasts. Maximum charge weights per 8 millisecond delay varied between 1.4 and 88 kg and scaled distances (SD) from 31.2 to 253.8 m/kg<sup>1/2</sup>. Peak Particle Velocities (PPV's) in the horizontal direction recorded in the ground outside at the structure ranged from 1 to 9 mm/s. Frequencies of the maximum excitation pulse varied between 3 Hz and 18 Hz. PPV's are well below the generally accepted threshold for cosmetic hairline cracks of 12 mm/s to 19 mm/s for excitation frequencies below 10 Hz. Airblast overpressures ranged from 0.002 to 0.02 kPa

Figure 2. Locations of crack and null sensors at the corner of the east window.

Both the S1 and S2 seismographs were connected to clusters of three single axis transducers in the upper and lower interior corners and adjoined wall at mid-wall (north or east wall) as shown in Figure 1. These transducers were affixed to the walls using hot glue to minimize damage during removal. The three corner transducers, labeled R, T, and V in Figure 1 (bottom, right), measured whole structure motions in the horizontal radial (nominal east-west), transverse (nominal north-south), and vertical directions, respectively. The mid-wall transducers measured horizontal motions during wall flexure or bending. Further details of this system can be found at (Aimone-Martin. et al, 2002)

To measure the effect of blasting and climate conditions (temperature and humidity) on changes in the width of an existing exterior crack, Kaman™ eddy-current gages were installed as shown in Figure 2 and data collected using a field computer. Each Kaman gage consisted of mounting brackets, an active element, and a target plate. Gages were mounted in brackets affixed to the stucco exterior across an existing crack (crack gage) and on an un-cracked surface (null gage). The crack gage was installed with each mounting bracket placed on either side of the crack. Operation of eddy-current gages has been described elsewhere (Dowding and Siebert, 2001 and Dowding and Snider, 2003, Hitz and Welsby, 1997).

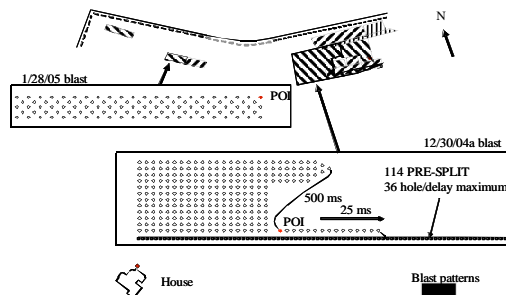


Figure 3. Typical trench shot pattern showing location relative to the structure and point of initiation (POI).

## 3 DYNAMIC CRACK AND STRUCTURAL RESPONSE

Nine time histories of excitation and response for blasts on 12/30a and 1/28 are shown in Figures 4 and 5. The upper three time histories are displacements of the crack and relative displacements

Table 1. Summary of blast details and measured ground and airblast.

Shot Date	Distance From Structure	Charge Weight/Delay	Scaled Distance	Peak Particle Velocity	Frequency at the PPV	Airblast	Number of holes	Shot Type
	(m)	(kg)	( $\text{mkg}^{1/2}$ )	( $\text{mm/sec}$ )	(Hz)	(kPa)		
9/16/2004	296	2.27	196.5	0.889	8.5	0.002	78	trench
9/17/2004	296	1.36	253.8	1.016	14.6	0.008	86	trench
9/21/2004	368	11.34	109.3	3.175	3.7	0.006	320	road cut
9/23/2004	299	3.40	162.2	1.143	14.2	0.002	360	trench
09/30/04	290	8.39	100.1	3.048	7.7	0.0012	290	road cut
12/30/04a	293	87.98	31.2	9.270	5.2	0.014	311/109 PS	road cut.PS
12/30/04b	293	18.14	68.8	3.175	4.5	0.006	48	road cut
1/27/05a	232	14.52	60.9	3.937	18.2	0.004	154	trench
1/27/05b	232	14.52	60.9	1.397	9.8	nd	42	trench
1/28/2005	257	22.68	54.0	3.683	10.2	0.02	103	trench

PS – pre -split shot detonated with road cut

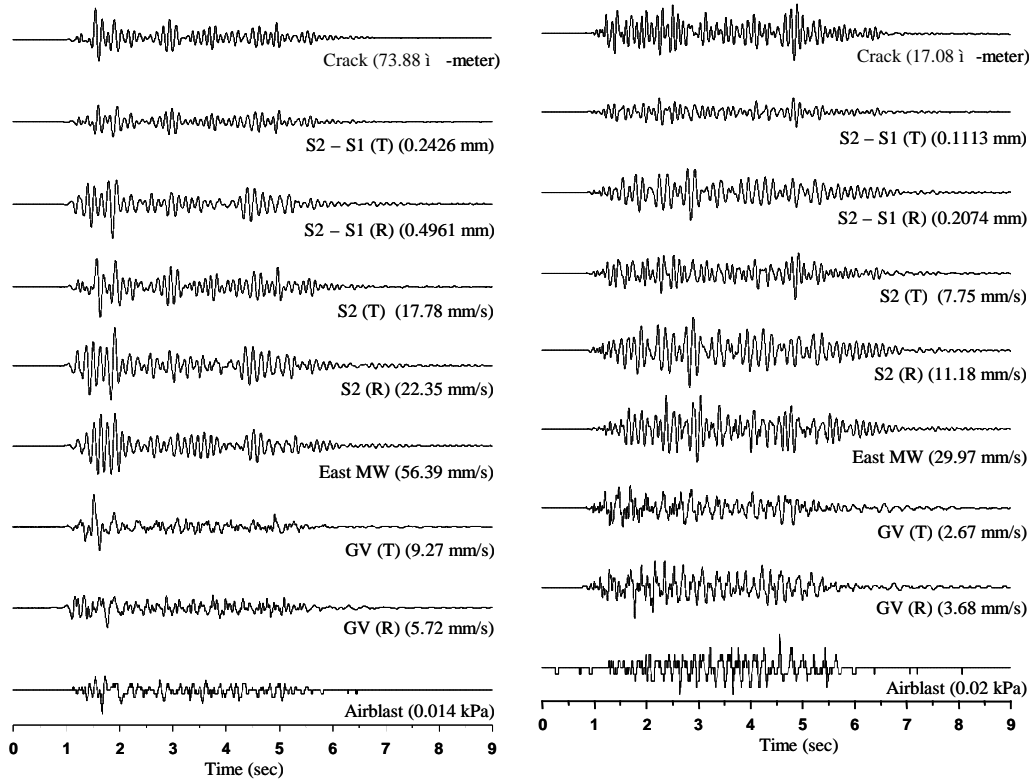


Figure 4. Time histories of structural response (upper five), excitation of ground velocities and air pressure and crack motions for event on 12/30/04a

Figure 5. Time histories of structural responses (upper five), excitation of ground velocities and air pressure and crack motions for event on 1/28/05.

between the upper and lower transducers in the radial & transverse directions. The next three below them are the velocity time histories of the response of the upper wall corners in the radial and transverse directions, and the mid-wall response (in the radial direction). The bottom three time histories are the excitation by air blast and radial and transverse ground motion. Transverse is parallel to the east wall containing the crack.

These two events produced the highest ground motions (12/30a) and the highest air blast overpressure (1/28). In neither case were the ground motion and air blast peaks separated in time enough to draw unequivocal conclusions. On 12/30, the peak air blast and ground motion occurred at the beginning of the time history and on 1/28, the peak air blast occurred near the end of the event while there was still significant ground motion. These two events involved the highest air blast overpressures of 0.02 kPa (120 dB or 0.003 psi) and 0.014 kPa (117 dB or 0.002 psi), which are relatively small compared to the allowable 0.07 kPa (133 dB or 0.01 psi).

The natural frequency of the structure can be estimated from the last several seconds (after second 6) of the radial structural motions excited by the 1/28 blast. These responses occur without significant ground motion or air blast excitation. S2 in the radial and the east mid-wall velocity responses are similar and indicate a natural frequency of some 8 Hz. Motions in the transverse direction are not as consistent but do contain significant motion in the same frequency range. During seconds 2-4, fairly uniform excitation occurs at a frequency of 6 Hz in both the radial and transverse directions. It is during this time that the maximum mid-wall and S2 radial response is observed

Peak responses (y-axes) are plotted in Figure 6 on the next page versus various excitation possibilities (x-axes). All points are the response peak (y) that follows the maximum excitation peak (x) by less than one response period. This comparison differs from finding the maximum peak response in the record first and then the preceding peak excitation within the preceding response period. The distinction is important as it allows observation of the significant drivers of response.

In Figure 6, the first row of graphs compare S2, velocity responses in the radial (perpendicular to the east wall containing the crack) transverse (parallel to the east wall) are compared with the time correlated maximum Peak Particle Velocity (PPV) in the same directions. In the second row, dynamic crack responses are compared with the maximum

PPV's in perpendicular and parallel to the wall containing the crack (radial and transverse directions respectively).

In the third row, dynamic crack responses are compared with maximum differential wall displacements between top (S2) and bottom (S1) transducers. Finally at the bottom peak crack responses are compared with the maximum air blast overpressures, which are omni-directional.

For this structure and range of excitation frequencies, the PPV in the direction parallel with the wall containing the crack (east wall) appears to be the best predictor of crack response. Row 2 comparison in Figure 6 show that the peak crack response is not predicted at all by the maximum radial ground motions (PPV direction perpendicular to the wall containing the crack). It is the transverse motions parallel with in-plane shearing that opens and closes the crack. The next closest predictor would be the differential displacement in the direction parallel to the east wall shown in the third row. However it is only a slightly better predictor than is the differential displacement in the perpendicular direction. Finally the air blast peak is the least able to predict the maximum crack response. The relatively small effect of the peak air blast overpressure may result from the small pressures generated at this test house by these events.

### 3 STRAINS

The magnitude of induced strains in structure components determines the likelihood of cosmetic cracking in residences. Global strains may be estimated from differential displacements at the upper, S2, and lower, S1, corners, in directions parallel and perpendicular to the plane of the wall of interest, the east wall in this case. Velocity time histories at S1 and S2 are first integrated to obtain displacement time histories, then the largest time correlated difference between corner responses (S2 - S1) is employed to calculate strain. Examples of such differential displacement time histories are presented as the second and third time histories from the top in Figures 4 and 5.

First consider differential displacements in the direction parallel to the east wall, which produce "in plane" shear and related tensile strains. Global shear strain is determined by the following:

$$\gamma_{\max} = \left( \frac{\delta_{\max}}{L} \right) \quad (1)$$

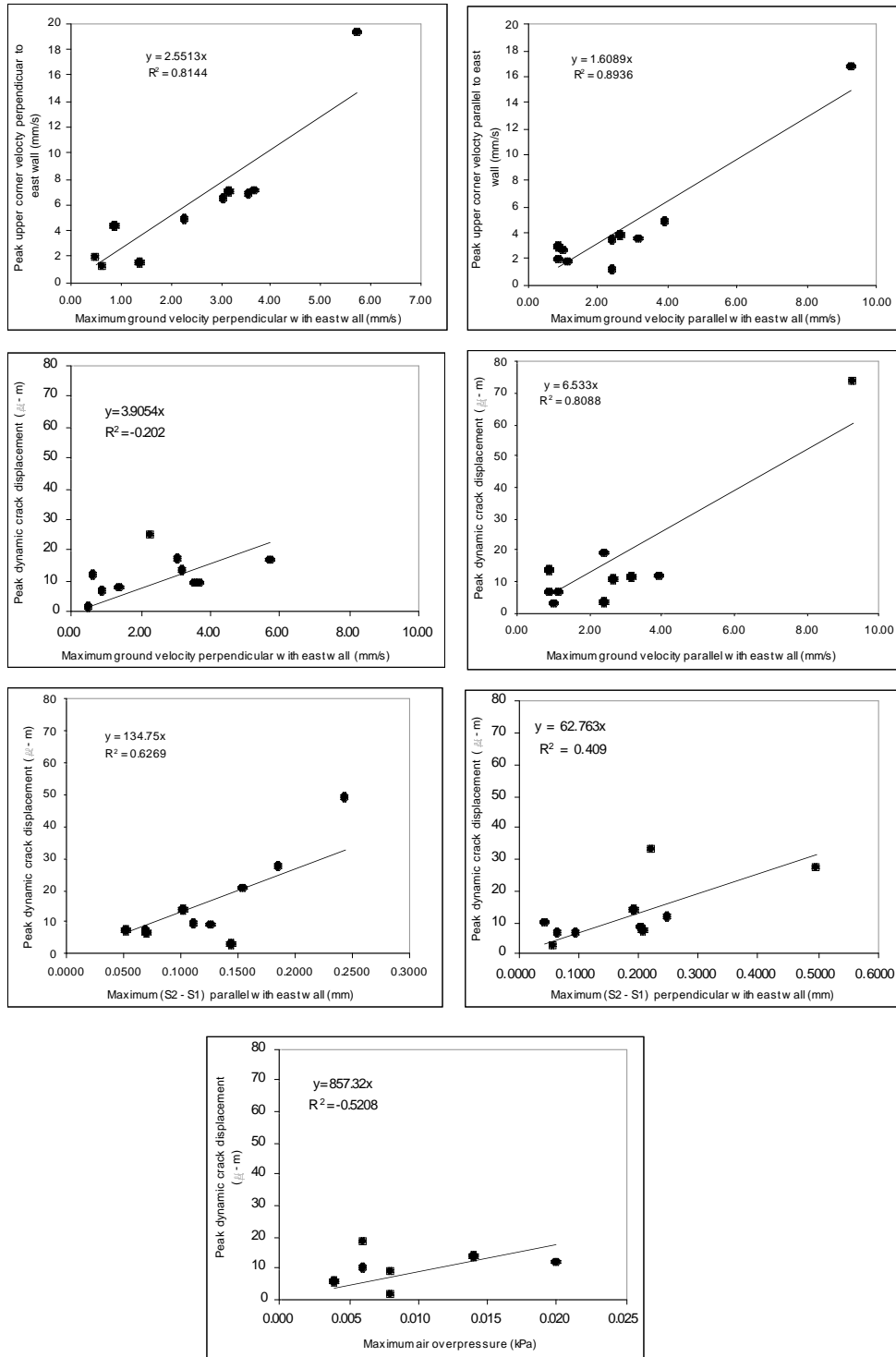


Figure 6. Structural and crack responses to peak ground motions, relative displacements, and airblast.

where  $\gamma_{\max}$  = global shear strain (micro-strains or  $10^{-6}$ );  $\delta_{\max}$  = maximum differential displacement parallel to the wall, S2 – S1 (in. or mm); L = height of the wall subjected to strain (in. or mm).

In-plane tensile strain,  $\epsilon_{L\max}$ , is calculated from global shear strain by the equation:

$$\epsilon_{L\max} = \gamma_{\max}(\sin\theta)(\cos\theta) \quad (2)$$

where  $\theta$  is the interior angle of the longest diagonal of the wall subjected to strain with reference to the horizontal. Theta,  $\theta$ , is calculated by taking the inverse tangent of the ratio of wall height to wall length.

Next consider differential displacements in the direction perpendicular to the east wall, which produce “out of plane” bending strains and the related extreme fiber tensile strains. While the lower wall, S1 is well coupled to the ground, or “fixed”, the upper wall, S2, and the roof can have varying degrees of “fixity”, ranging from relatively unconstrained to highly fixed. Bending strain is most conservatively estimated with the fixed-fixed analogy because this mode shape predicts the highest strains in walls per unit of maximum relative displacement (Dowding, 1996). These out of plane bending strains can be calculated as:

$$\epsilon = \left( \frac{d6\delta_{\max}}{L^2} \right) \quad (3)$$

where  $\epsilon$  = bending strain in walls (micro-strains or  $10^{-6}$ ); d = the distance from the neutral axis to the wall surface, or one half the thickness of the wall subjected to strain (in. or mm).

Table 2 summarizes maximum calculated strains induced by ground motion excitation. The maximum recorded whole structure differential displacement was 0.4961 mm in the plane of the east wall containing the crack. Maximum, calculated, in-plane global shear strains and related tensile strains were 135 and 67 micro strain. The maximum calculated, out of plane bending strain was 38 micro-strains. The range of failure in the gypsum core of drywall is 300 to 500 micro-strains (Dowding, 1996). Using the maximum observed tensile strain of 67, the factors of safety against cracking were 4 to 7 for the interior drywall. Therefore, any cracks in interior drywall cannot be attributed to blasting strains.

Table 2. Calculated wall strains compared with maximum ground velocities and crack motions

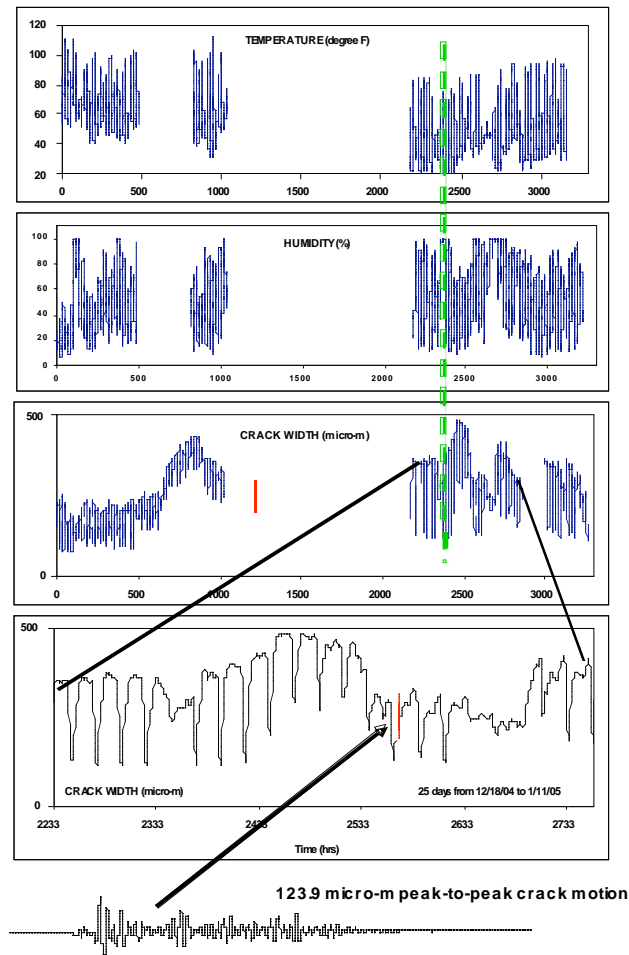
Shot Date	Maximum differential wall displacement, S2-S1 (mm)		Maximum shear strain (micro-strain)	Maximum in-plane tensile strain (micro-strain)	Maximum bending strain (micro-strain)	Maximum ground velocity (mm/s)		Peak Crack Motion (micro-m)
	perpendicular to east wall	parallel to east wall	east wall	east wall	east wall	Radial	Transverse	
9/16/2004	0.04369	0.06937	11.94	5.94	3.99	0.635	0.889	18.67
9/17/2004	0.05733	0.14406	15.67	7.79	4.63	0.508	1.016	6.33
9/21/2004	0.19285	0.10249	28.02	26.22	12.52	3.175	2.413	19.72
9/23/2004a	0.09627	0.05179	26.32	13.09	6.74	0.889	1.143	14.13
09/30/04	0.24890	0.12602	68.05	33.84	18.00	3.048	2.413	20.69
12/30/2004a	0.49607	0.24261	135.63	67.44	38.44	5.715	9.271	73.89
12/30/2004b	0.20403	0.15352	55.78	27.74	14.78	2.286	3.175	25.07
1/27/2005a	0.22157	0.18476	60.56	30.12	16.07	3.556	3.937	34.65
1/27/2005b	0.06573	0.06974	17.97	8.94	4.40	1.397	0.889	10.69
1/28/2005	0.20744	0.11113	56.7	28.2	18.25	3.683	2.667	17.09

#### 4 LONG-TERM OR ENVIRONMENTAL AND WEATHER INDUCED CRACK RESPONSE

Long-term changes in crack width are presented in Figure 7 along with outside temperature and humidity for a period of 135 days (3240 hours). In general, long-term crack movement followed the trend in exterior humidity while short-term (or 24 hour) movement was consistent with diurnal temperature. When the humidity increased, the crack opened (positive change) whereas a sudden increase in temperature produced crack closure.

Weather front effects such as rain (shown with the vertical dashed line in Figure 7) had the largest influence on long-term crack movements. In contrast, daily crack movements were strongly affected by the early morning sun on the eastern wall exposure. The large variation in crack width over a ½ day cycle can be seen in the graphical expansion of hours 2233 to 2760. The largest measured change over this daily cycle was some 300 micro-meters.

Peak to peak dynamic crack motions (red bar) from the most significant blast on 12/30/04a are compared with daily and long term environmental effects bottom two graphs in Figure 7.



**73.9 micro-m maximum zero-to-peak crack displacement**

Figure 7. Comparison of long term crack response with outside temperature and humidity showing relative dynamic crack motions during the blast on 12/30/04a.

The daily change of 300 micro-meters (peak to peak) exceeded the largest change in crack width

during blasting (74 micro-meters zero to peak and 124 peak to peak) on 12/30/04a. Furthermore, the greatest overall change in crack width for the duration of the study was 410 micro-meters as shown on the 133 day portion of Figure 7. This weather-induced change in crack width is the largest contributing factor to crack extension and widening over time. Blasting vibration influence on changes in crack widths are negligible compared with the influence of climate. Hence, blasting is unlikely to be the source of stucco cracking.

It is important to measure crack response for several months to observe the long-term environmental effects. As shown in Figure 7, despite significant diurnal solar heating on the east wall, the longer term or seasonal effects were still larger (300 and 410 micro-meters, respectively).

## 5 CONCLUSIONS

Peak airblast levels did not occur at the same time as peak crack and structure response and thus under predicts response. This lack of influence may result from the low level of air blast generated in this study at the test structure. Similar studies at higher air blast overpressure levels are needed.

On the other hand peak ground motion levels did occur slightly ahead of the peak crack and structure response, and were better predictors of crack response than were air blast overpressures.

Natural frequency of the structure was determined from free vibration response as 8 Hz, which is within the expected range of 4 Hz to 12 Hz.

Calculated maximum in-plane tensile wall strain from ground motion excitations was 67 micro-strains. Calculated maximum mid-wall bending strain was 38 micro-strains. Maximum airblast induced mid-wall bending strains could not be distinguished. These blast-induced strains are far less than the 300 to 500 micro-strains necessary to fail dry wall.

Crack response to environmental changes was far greater than response to dynamic excitation from either ground motions or air blast overpressures. The maximum recorded crack width response from blasting was 74 and 123 micro-meters zero to peak and peak to peak respectively. During the 133 day study daily temperature and humidity induced crack peak to peak responses of up to 300 micro-meters, and the seasonal environmental effects induced crack responses of 410 micro meters.

## 6 ACKNOWLEDGEMENTS

This project was sponsored and supported by Salls Brothers Construction, Inc. The authors acknowledge the guidance and contributions of John White of Salls and students participating on this project from Northwestern University and New Mexico Institute of Mining and Technology. Crack Monitoring equipment was supplied by the Infrastructure Technology Institute at Northwestern University, which supported by a block grant from the US DOT to commercialize innovative instrumentation. More information on Autonomous Crack Monitoring instrumentation is available on the internet from [www.iti.northwestern.edu/acm](http://www.iti.northwestern.edu/acm).

## 7 REFERENCES

Aimone-Martin, C.T., M.A. Martell, L.M. McKenna, D.E. Siskind, and C.H. Dowding (2002), Comparative Study of Structure Response to Coal Mine Blasting, Report prepared for the United States Office of Surface Mining Reclamation and Enforcement, Pittsburgh, PA, USA. Available at [www.osmre.gov/blastingindex.htm](http://www.osmre.gov/blastingindex.htm).

Dowding, C.H. (1996) Construction Vibrations, originally published by Prentice Hall, NJ, USA, reprints now available at Amazon.com 620 pgs.

Dowding, C.H. and Sinder, M. (2003) "New Approach to Control of Vibrations Generated by Construction in Rock and Soil", *Proceedings of the Soil and Rock America Symposium*, the 12th Pan American Conference on Soil Mechanics and Geotechnical Engineering and the 39th US Rock Mechanics Symposium, Massachusetts Institute of Technology (MIT), VGE, Essen Germany. Reprints of article available at [www.iti.northwestern.edu/acm](http://www.iti.northwestern.edu/acm).

Dowding C.H. and Siebert, D. (2001) "Control of Construction Vibrations with an Autonomous Crack Comparometer" *Proceedings of the Conference on Explosives and Blasting Technique*, European Federation of Explosives Engineers, Munich, Germany, AA Balkema. Reprints of article available at [www.iti.northwestern.edu/acm](http://www.iti.northwestern.edu/acm)

Hitz, T. and S.D. Welsby, 1997, True Position Measurement with Eddy-Current Technology, *Sensors Magazine*, pp. 13.